ELSEVIER

Synthesis and characterization of methylbismuth(III) complexes containing dithio ligands: 2. Crystal and molecular structure of [MeBiCl(S$_2$CNEt$_2$)] and transformation of some [MeBi(S$_2$CNR$'_2$)$_2$] to Bi$_2$S$_3$

Amit K. Jain [a], Vinita Sharma [a], Rakesh Bohra [a,*], A.A. Sukumar [b], V.S. Raju [b], John E. Drake [c], Michael B. Hursthouse [d], Mark E. Light [d]

[a] *Department of Chemistry, University of Rajasthan, Jaipur 302004, India*
[b] *National Centre for Compositional Characterisation of Materials, Bhabha Atomic Research Centre, Hyderabad 500062, India*
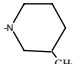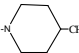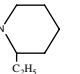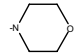[c] *Department of Chemistry and Biochemistry, University of Windsor, Windsor, Canada ON N9B 3P4*
[d] *Department of Chemistry, University of Southampton, Highfield, Southampton SO17 11BJ, UK*

Abstract

Reactions of methylbismuth(III) dichloride with sodium salts of dithiocarbamates have been carried out in 1:1 and 1:2 stoichiometric ratios in anhydrous benzene to yield products of the types [MeBiCl(S$_2$CNR$_2$)] [where R = Me (**1**), Et (**2**) and ^{i}Pr (**3**)] and

[MeBi(S$_2$CNR$'_2$)$_2$] [where NR$'_2$ = (**4**), (**5**), (**6**), (**7**) and (**8**)].

These complexes were characterized by elemental analyses and by FT-IR and NMR (^{1}H and ^{13}C) spectra. The X-ray structure of [MeBiCl(S$_2$CNEt$_2$)] (**2**), indicates the presence of unique Bi···Cl···Bi secondary bonds resulting in a distorted square pyramidal environment around the central bismuth(III) atom. TGA of (**6**) shows a single step break down of the complex to Bi$_2$S$_3$ at 262.8 °C. Transformations of (**6**) and (**8**) to pure Bi$_2$S$_3$ have been carried out successfully in refluxing xylene (142 °C) as revealed by XRD and SEM studies.
© 2006 Elsevier B.V. All rights reserved.

Keywords: Methylbismuth(III); Dithioligands; NMR; Crystal structure; XRD; SEM and TGA

1. Introduction

Sustained interest in the chemistry of bismuth(III) chalcogenides is due to their increasing applications in solar cells, photolithiography, optical memory devices and as photo-and thermo-electric conductors [1,2]. Therefore, it is not surprising that the chemistry of bismuth(III) derivatives with xanthates, dithiocarbamates and alkyl – as well as alkylene-dithiophosphate based ligands has been an active area of research for a long time. The catalytic and biocidal applications of dithio derivatives of bismuth(III) are very well documented [3,4]. The interest is not only due to their facile transformation to Bi$_2$S$_3$ at low temperatures as compared to the traditional high sintering temperature methods, but also due to their tendency to exhibit interesting structural variations ranging from monomeric to polymeric supramolecular assemblies [5,6].

Our previous studies [7] on the synthesis and characterization of a single source molecular precursor for Bi$_2$S$_3$, led us to the preparation of some novel methylbismuth(III) derivatives of dithio ligands exhibiting interesting structural features (Fig. 1).

* Corresponding author. Tel./fax: +91 141 2700364.
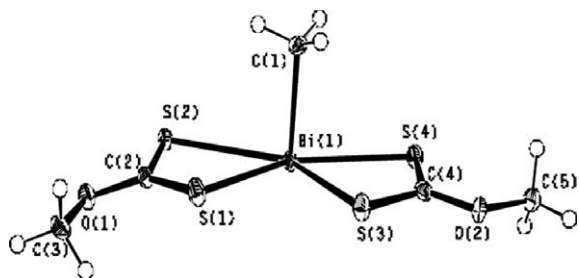 *E-mail address:* rkbohra@satyam.net.in (R. Bohra).

Fig. 1.

In continuation of the above, we report herein the synthesis and characterization of methylbismuth(III) derivatives with simple and heterocyclic dithiocarbamates. The structure of one of the compounds [MeBiCl(S$_2$CNEt$_2$)] (**2**) has been established by single crystal X-ray diffraction. On refluxing xylene solution of (**6**) and (**8**) separately, formation of pure Bi$_2$S$_3$ was observed.

2. Experimental

All manipulations involving the preparations of dithiocarbamates [8] and methylbismuth dichloride [9] were carried out under anhydrous and inert conditions. IR spectra were recorded as Nujol mulls between CsI plates in the range 4000–200 cm^{-1}. The ^{1}H and ^{13}C{^{1}H} NMR spectra were recorded in 5 mm NMR tubes, on a Bruker DPX-300 spectrometer operating at 300 and 75.47 MHz, respectively. Chemical shifts are relative to internal chloroform (δ 7.26 ppm) for ^{1}H and (δ 77.0 ppm) for ^{13}C. Microanalyses were performed on a Heraeus Carlo Erba 1108 analyzer.

2.1. Preparation of [MeBiCl(S$_2$CNEt$_2$)] (2)

Solid NaS$_2$CNEt$_2$ (426 mg, 2.49 mmol) was added to a stirred benzene suspension ($\sim$30 ml) of MeBiCl$_2$ (733 mg, 2.49 mmol). The whole reaction mixture was stirred for 5 h and filtered. The solvent was stripped off in *vacuo* to

Table 1
Synthetic and analytical data of [MeBiCl(S$_2$CNR$_2$)]

S. No.	Complexes	Yield (%)	Physical state and colour	Analysis found (Calcd.)			
				N	S	Cl	Bi
1	MeBiCl(S$_2$CNMe$_2$)	55	Yellow paste	3.5 (3.7)	16.6 (16.9)	9.3 (9.3)	54.8 (55.0)
2	MeBiCl(S$_2$CNEt$_2$)	60	Yellow solid	3.2 (3.4)	15.4 (15.7)	8.5 (8.7)	51.0 (51.3)
3	MeBiCl(S$_2$CN^{i}Pr$_2$)	82	Yellow solid	3.1 (3.2)	14.4 (14.7)	8.0 (8.1)	47.7 (47.9)

Table 2
Synthetic and analytical data of [MeBi(S$_2$CNR$'_2$)$_2$]

S. No.	Complexes	Yield (%)	Physical state and colour	Analysis found (Calcd.)					m.p. (°C)
				C	H	N	S	Bi	
4	NR$_2$'= -N⬡	59	Yellow solid	28.5 (28.7)	4.3 (4.3)	4.9 (5.1)	23.3 (23.6)	37.8 (38.4)	138 (dec.)
5	NR$_2$' = -N⬡CH$_3$	97	Orange solid	31.2 (31.5)	4.6 (4.8)	4.8 (4.9)	22.0 (22.4)	36.3 (36.5)	90
6	NR$_2$' = -N⬡-CH$_3$	99	Yellow solid	31.3 (31.5)	4.5 (4.8)	4.6 (4.9)	22.0 (22.4)	36.2 (36.5)	84
7	NR$_2$' = -N⬡C$_2$H$_5$	97	Yellow solid	33.6 (34.0)	5.0 (5.2)	4.5 (4.7)	21.0 (21.4)	34.5 (34.8)	78
8	NR$_2$' = -N⬡O	68	Yellow solid	23.9 (24.1)	3.2 (3.5)	5.0 (5.1)	23.0 (23.4)	38.0 (38.1)	96

afford a yellow solid in 60% yield. Other monochloromethylbismuth(III) derivatives were prepared in a similar manner (Table 1).

2.2. Preparation of [MeBi{S₂C-N⟨⟩-CH₃}₂] (**6**)

Solid ligand (1.08 g, 5.48 mmol) was added to a stirred benzene suspension (∼30 ml) of MeBiCl₂ (800 mg, 2.73 mmol). The whole reaction mixture was stirred for 5 h at room temperature and precipitated NaCl was filtered off. The excess solvent was removed under reduced pressure to give a yellow solid in 99% yield, which was recrystalized from dichloromethane-*n*-hexane mixture. Similarly other bis(dithiocarbamato)methylbismuth(III) complexes were prepared (Table 2).

2.3. Pyrolysis of complexes [MeBi{S₂C-N⟨⟩O}₂] (**8**)

A xylene solution of the complex (**8**) was refluxed for 2 h under N₂ atmosphere. A gray black material was obtained. The supernatant was decanted and the residue was washed with chloroform (2×10 ml) and further with *n*-hexane (2×10 ml). Finally, dried under reduced pressure and identified as pure Bi₂S₃ from its XRD pattern (Fig. 2). Analysis: C, 0.6%; H, 0.2%. A similar procedure was used for the pyrolysis of complex (**6**).

2.4. X-ray diffraction analysis

X-ray diffraction data of a colourless crystal of [MeBiCl(S₂CNEt₂)] were collected on an Enraf Nonius KappaCCD diffractometer, with ϕ and ω scans chosen to give a complete asymmetric unit. Cell refinement [10] gave cell constants corresponding to a monoclinic cell. An absorption correction was applied [10]. Cell parameters are summarized in Table 3. The structure was solved by

direct methods [11] and was refined using the WINGX version [12] of SHELX-97 [13]. All of the non-hydrogen atoms were treated anisotropically. Hydrogen atoms were included in idealized positions with isotropic thermal parameters set

Table 3
Crystal data and structure refinement for [MeBiCl(S₂CNEt₂)]

Empirical formula	C₆ H₁₃ N S₂ Cl Bi
Formula weight	407.72
Temperature (K)	120(2)
Wavelength (Å)	0.71069
Crystal system	monoclinic
Space group	$P2_1/c$
Unit Cell Dimensions	
a (Å)	9.973(5)
b (Å)	7.941(5)
c (Å)	14.656(5)
β (°)	105.045(5)
V (Å³)	1121(1)
Z	4
D_{calc} (g cm⁻³)	2.416
Absorption coefficient (mm⁻¹)	16.286
$F(000)$	752
Crystal size (mm³)	$0.20 \times 0.15 \times 0.03$
θ Range for data collection (°)	3.86 to 27.47
Index ranges	$-12 \times h \times 12$, $-9 \times k \times 10$, $-18 \times l \times 19$
Reflections collected	9176
Independent reflections	2519 ($R_{int} = 0.0528$)
Max. and min. transmission	0.6408 and 0.1391
Refinement method	Full-matrix least-squares on F^2
Data/restraints/parameters	2519/0/104
Goodness-of-fit on F^2	1.059
Final R indices ($F^2 > 4\sigma(F^2)$)	$R_1 = 0.0349$, $wR_2 = 0.0828$
R indices (all data)	$R_1 = 0.0424$, $wR_2 = 0.0874$
Extinction coefficient	0.0037(4)
Largest difference in peak and hole (e Å⁻³)	2.791 and −3.633

Fig. 2. XRD pattern of Bi₂S₃ obtained from complex **6** by refluxing in xylene.

Table 4
Bond lengths (Å) and bond angles (°) for [MeBiCl(S₂CNEt₂)]

Bond lengths			
Bi(1)–S(1)	2.670(2)	Bi(1)–S(2)	2.679(2)
Bi(1)–C(1)	2.228(6)	Bi(1)–Cl(1)	2.895(2)
Bi(1)–Cl(1)′	2.918(2)	Cl(1)–Bi(1)″	2.918(2)
S(1)–C(2)	1.743(6)	S(2)–C(2)	1.734(6)
N(1)–C(2)	1.311(8)	N(1)–C(3)	1.484(8)
N(1)–C(5)	1.481(7)	C(3)–C(4)	1.51(1)
C(5)–C(6)	1.52(1)	Bi(1)—Bi(1)′	4.3121(4)

Bond angles			
C(1)–Bi(1)–S(1)	92.9(2)	C(1)–Bi(1)–S(2)	94.3(2)
C(1)–Bi(1)–Cl(1)	84.1(2)	C(1)–Bi(1)–Cl(1)′	84.1(2)
S(1)–Bi(1)–S(2)	67.17(5)	Cl(1)–Bi(1)–Cl(1)′	138.58(4)
S(1)–Bi(1)–Cl(1)	75.17(5)	S(2)–Bi(1)–Cl(1)′	78.27(5)
Cl(1)–Bi(1)–S(2)	142.19(5)	Cl(1)′–Bi(1)–S(1)	145.00(5)
Bi(1)–Cl(1)—Bi(1)″	95.77(5)	Bi(1)—Cl(1)′–Bi(1)′	95.77(5)
C(2)–S(1)–Bi(1)	88.2(2)	C(2)–S(2)–Bi(1)	88.1(2)
S(2)–C(2)–S(1)	116.6(4)	C(2)–N(1)–C(3)	121.8(5)
C(2)–N(1)–C(5)	122.1(5)	C(5)–N(1)–C(3)	116.1(5)
N(1)–C(2)–S(1)	121.6(5)	N(1)–C(2)–S(2)	121.7(5)
N(1)–C(3)–C(4)	111.9(5)	N(1)–C(5)–C(6)	111.5(5)

Equivalent positions ($-x$, $y - 1/2$, $-z + 1/2$) given by a prime and ($-x$, $y + 1/2$, $-z + 1/2$) by a double prime.
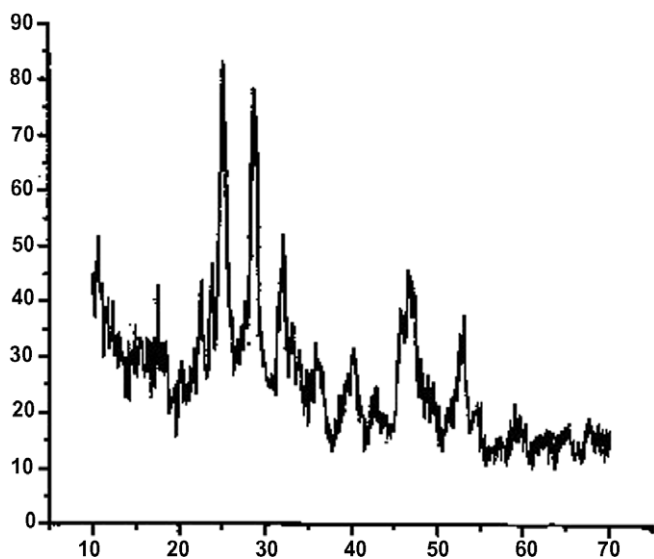
at 1.2 times that of the carbon atom to which they were attached. The final cycle of full-matrix least-squares refinement was based on 2519 observed reflections (2207 for $F^2 > 4\sigma(F^2)$) and 104 variable parameters and converged (largest parameter shift was 0.001 times its esd). The relatively high residual peaks are not unusual in view of the slab-like shape of the small crystal combined with the presence of the heavy atom.

Distances and bond angles are given in Table 4. The immediate environment around bismuth is displayed as an ORTEP diagram in Fig. 3, and the polymeric nature of the molecule in Fig. 4. Additional material available from Cambridge Crystallographic Data Centre comprises the final atomic coordinates and thermal parameters for
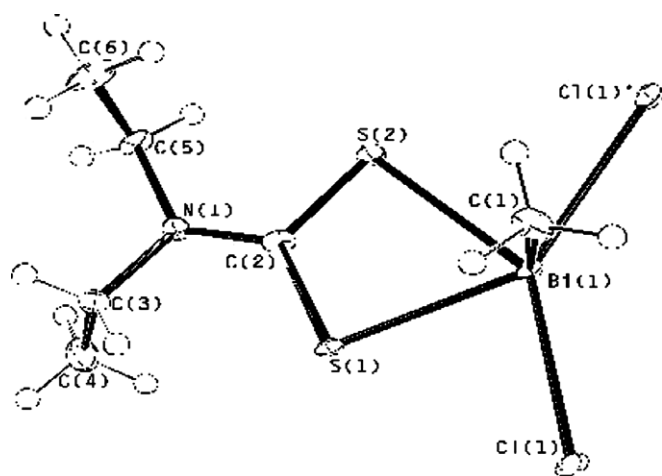

Fig. 3. Ortep plot showing the immediate environment around bismuth in [MeBiCl(S$_2$CNEt$_2$)].

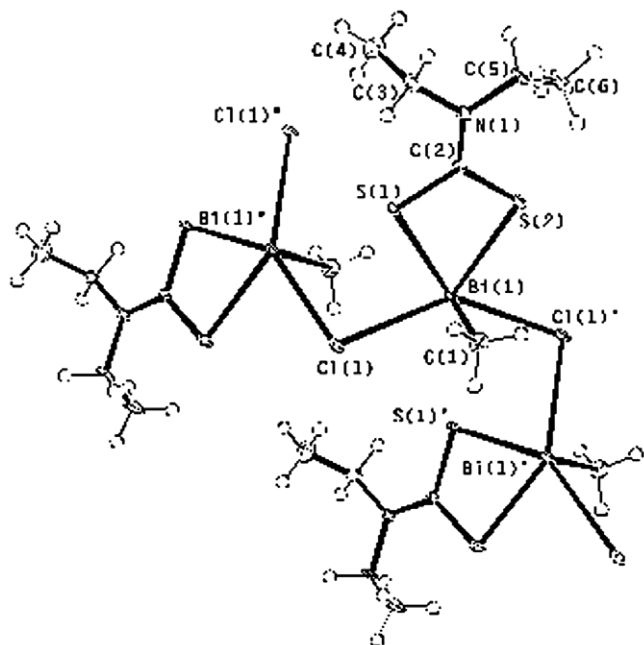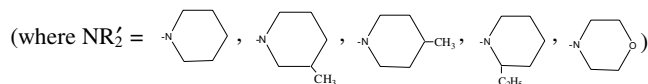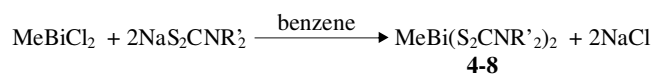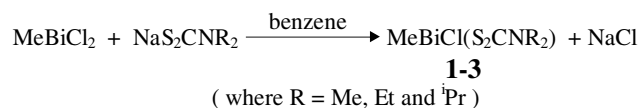

Fig. 4. Ortep plot showing extended polymeric structure of [MeBiCl(S$_2$CNEt$_2$)].

all atoms and a complete listing of bond distances and angles.

3. Result and discussion

3.1. Synthesis

Reactions of MeBiCl$_2$ with the sodium salts of dithiocarbamates in different stoichiometric ratios in anhydrous benzene gave products of the types [MeBiCl(S$_2$CNR$_2$)] and MeBi(S$_2$CNR$'_2$)$_2$ as depicted below:

$$MeBiCl_2 + NaS_2CNR_2 \xrightarrow{benzene} MeBiCl(S_2CNR_2) + NaCl$$
$$\mathbf{1\text{-}3}$$
(where R = Me, Et and ^{i}Pr)

$$MeBiCl_2 + 2NaS_2CNR'_2 \xrightarrow{benzene} MeBi(S_2CNR'_2)_2 + 2NaCl$$
$$\mathbf{4\text{-}8}$$

(where NR$'_2$ = ...)

Except for **1** (yellow paste) all of these complexes are yellow–orange solids and are found to be thermally unstable at room temperature (Tables 1 and 2). The monochloro derivatives (**1**–**3**) have poor solubility in common organic solvents and the solubility decreases with the decrease in steric size of the N–R group (Pr^i > Et > Me). In contrast to this bis(dithiocarbamato)methylbismuth(III) complexes (**4**–**8**) are found to be soluble in common organic solvents. Elemental analyses corresponded to the expected formula.
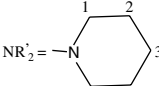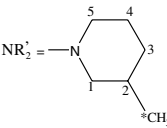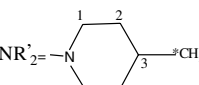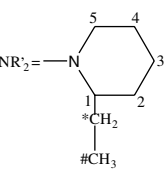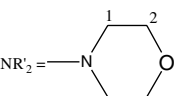
3.2. IR spectra

The assignment of IR bands was made by comparison to the literature and the spectrum of starting material. A weak to medium intensity band in the region 246–272 cm^{-1} has been assigned to ν(Bi–S) [14] while a medium to strong intensity band in the region 426–469 cm^{-1} has been assigned to ν(Bi–C) [14]. These derivatives also show medium to strong intensity bands in the region 1427–1438 cm^{-1} and 1000–1081 cm^{-1} assigned to ν(C=N) and ν(C=S) stretching vibrations, respectively, consistent with the biconnective nature of the dithiocarbamate moieties in these complexes.

3.3. NMR spectra

The NMR spectra were recorded in CDCl$_3$ and the data are summarized in Table 5. In the ^{1}H NMR spectra, the Me–Bi protons are deshielded and appeared as a single resonance in the region δ 2.14–2.37 ppm (MeBiCl$_2$, δ

Table 5
^1H and ^{13}C NMR (in δ ppm) spectral data of the complexes, [MeBiCl(S$_2$CNR$_2$)] (1–3) and [MeBi(S$_2$CNR$'_2$)$_2$] (4–8)

S. No.	Complexes	^1H NMR	^{13}C NMR
1	R = Me	1.52 (s, ▲); 2.37 (s, Me–Bi); 3.27 (s, ▲); 4.20 (s, NMe$_2$)	–
2	R = Et		–
3	R = ^{i}Pr	1.56 (d, 21 Hz, CHMe$_2$); 1.77(s, ▲); 2.37 (s, Me–Bi); 2.57 (s, ▲); 4.18 (m, NCH)	–
4	NR'$_2$ = piperidine ring (N, positions 1, 2, 3)	1.67–1.99 (br, H-3); 2.14 (s, Me–Bi); 3.99-4.03 (br, H-1 & H-2).	24.2 (C-3); 25.6 (C-2); 41.8 (C-1); 51.3 (Me–Bi); 199.9 (CS$_2$)
5	NR'$_2$ = methyl-substituted ring (positions 1, 2, 3, 4, 5, *CH$_3$)	0.95 (d, 6.6 Hz(d), H-*); 1.77–1.89 (m, H-4); 2.20 (s, Me–Bi); 2.66–2.76 (m, H-2); 3.03 (td, 12.3 Hz(t), 3.0 Hz(d), H-3); 4.18 (d, 6 Hz, H-1); 4.88 (t, 14.7 Hz(t), H-5)	18.7 (C-*); 24.9 (C-4), 31.4 (C-2); 32.9 (C-3); 51.0 (Me–Bi); 54.3 (C-1); 57.6 (C-5); 200.0(CS$_2$)
6	NR'$_2$ = methyl-substituted ring (positions 1, 2, 3, *CH$_3$)	0.96 (d, 6.1 Hz(d), H-*); 1.30 (q, 10.7 Hz(q), H-2); 1.70–1.78 (m, H-3); 2.19 (s, Me–Bi); 3.03 (t, 11.9 Hz(t), H-1)	21.3 (C-*); 30.8 (C-2); 33.7 (C-3); 50.9 (Me–Bi & C-1); 199.7 (CS$_2$)
7	NR'$_2$ = ethyl-substituted ring (positions 1, 2, 3, 4, 5, *CH$_2$, #CH$_3$)	0.92 (t, 7.4 Hz(t), H-*); 1.62–1.92 (m, H-#, H-2, H-3 & H-4); 2.24 (s, Me–Bi); 3.04 (t, 12.3 Hz(t), H-5); 5.19 (br, H-1)	10.6 (C-*); 18.8 (C-#); 22.9 (C-3); 25.3 (C-2); 27.3 (C-4); 45.5 (C-5); 47.4 (Me–Bi); 59.6 (C-1); 199.4 (CS$_2$)
8	NR'$_2$ = morpholine ring (N, O, positions 1, 2)	2.17 (s, Me–Bi); 3.76 (t, 4.7 Hz(t), H-1); 4.11 (t, 4.7 Hz(t), H-2)	50.0 (Me–Bi); 59.8 (C-1); 65.9 (C-2); 201.8 (CS$_2$)

▲, unassigned signals.

1.57 ppm). The N–R protons of simple dithiocarbamate derivatives (1–3) and the ring protons of the heterocyclic dithiocarbamates (4–8) appeared with expected multiplicities at the appropriate positions and integration in the ^1H NMR spectra of these complexes. Due to the very poor solubility of the monochloromethylbismuth(III) derivatives (1–3), their ^{13}C NMR spectra could not be obtained. For complexes (4–8), in ^{13}C NMR spectra, the Me–Bi carbon signal appeared in the region δ 47.4–51.3 ppm. All these compounds displayed a signal at δ 199.4–201.8 ppm due to –NCS$_2$ carbon resonances. In addition, all these derivatives also exhibited the expected signals due to ring carbon atoms (Table 5).

3.4. XRD pattern

The thermal behavior of two representative compounds (6) and (8) has also been studied for the preparation of pure Bi$_2$S$_3$. These complexes, when refluxed separately for 2 h in xylene under inert media, both yielded blackish gray powders, which were identified as pure Bi$_2$S$_3$ from microanalyses, XRD pattern (Fig. 2) [15] and IR spectra. The scanning electron micrograph of these products (Fig. 5(a,b)) taken at different resolutions showed agglomerated particles made up of nanosized grains.

3.5. Thermo gravimetric analysis

The TG curve (Fig. 6) of complex 6 showed a single step decomposition finally leading to the formation of pure bismuthinite, Bi$_2$S$_3$ from 55.7% weight loss.

3.6. X-ray crystal structure of [MeBiCl(S$_2$CNEt$_2$)] (2)

The immediate environment around bismuth is distorted square pyramidal (Fig. 3). The methyl group is out of the approximate plane formed by the two Cl atoms, Bi(1)–Cl(1) (2.895(2) Å) and Bi(1)–Cl(1)′ (2.918(2) Å), respectively, and the two S atoms of the bidentate ligand. In the related species, MeBi(S$_2$CNEt$_2$)$_2$ [16], the plane is formed
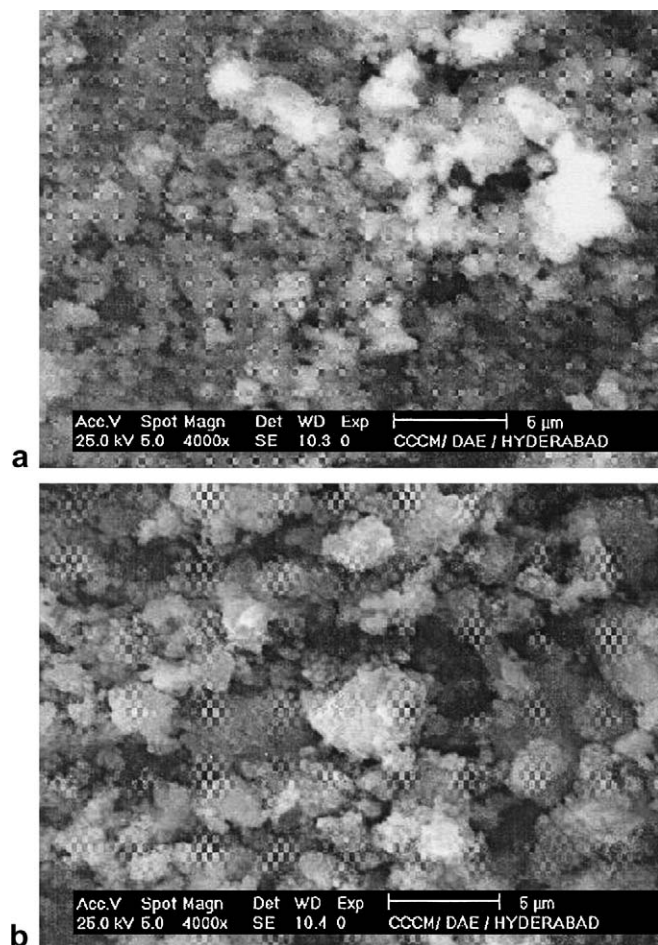
2.907(16) Å is similar to that of the longer Bi–S bonds in MeBi(S$_2$CNEt$_2$)$_2$ [16]. The bond to the methyl group in the vertical position Bi(1)–C(1) (2.228(6) Å) is short relative to the sum of the covalent radii of Bi and C of 2.37 Å, as was the case for MeBi(S$_2$CNEt$_2$)$_2$ [16] and MeBi(S$_2$COMe)$_2$ [7]. In **2**, the C–Bi–S angles of 92.9(2) and 94.3(2)° are comparable with the corresponding C–Bi–S angles involving the shorter Bi–S bonds in MeBi(S$_2$CNEt$_2$)$_2$ [16] ranging from 90.7(1) to 94.8(1)°, while the two C–Bi–Cl angles are both 84.1(2)° in contrast to the C–Bi–S angles involving the longer Bi–S bonds in MeBi(S$_2$CNEt$_2$)$_2$ [16] which range from 80.4(1) to 88.6(1)°. In the xanthate derivative MeBi-(S$_2$COMe)$_2$ [7], the C–Bi–S angles range from 86.8(2) to 92.0(2)°, but without an obvious correlation to the Bi–S bond lengths. The bite angles of the ligands in MeBi-(S$_2$CNEt$_2$)$_2$ (ave 62.93(4)°) and in MeBi(S$_2$COMe)$_2$ (62.06(4) and 64.70(4)°) are smaller than in **2** (67.17(5)°). This bite angle along with the angles Cl(1)–Bi(1)–Cl(1)′ = (138.58(4)°), S1–Bi(1)–Cl(1) (75.17(5)°) and S(2)–Bi(1)–Cl(1)′ (78.27(5)°) sum to 359°.

A distinctive feature in the solid state structure of MeBiCl(S$_2$CNEt$_2$) (**2**) (Fig. 4) is the bridging provided by the two chlorine atoms to give relatively strong Bi—Cl—Bi interactions resulting in an infinite chain with Bi(1)″–Cl(1)–Bi(1) and Bi(1)–Cl(1)′–Bi(1)′ angles of 95.77(5)°, resulting in the shortest Bi···Bi distance of 4.3121(4) Å.

It was noted in MeBi(S$_2$COMe)$_2$ [7] that the space between S(2) and S(4) was occupied by the sulfur atom of an adjacent molecule to give an intermolecular bond, Bi(1)—S(2)′, whose length of 3.253(1) Å was much closer to that of the longest ligand bond than to the sum of the van der Waal radii of Bi and S of *ca*. 4.0 Å. Thus, the environment around Bi could be considered to be a distorted pentagonal pyramid in the solid state to give an extended polymeric structure with the sulfur of the longest Bi–S bond acting as a bridge with a Bi(1)—S(2)′–Bi(1)′ angle of 140.46(3)°. In a similar fashion, the space between Cl(1) and Cl(1)′ is occupied by the sulfur atom of an adjacent molecule but the distance of Bi(1)—S(1)′ (3.543(2) Å) is considerably longer suggesting, at best, very weak intermolecular interactions and hence less reason to consider a distorted pentagonal pyramidal environment about bismuth.

4. Conclusion

The synthesis and characterization of methylbismuth(III) derivatives with dithiocarbamates in different stoichiometric ratios have been carried out to afford

Fig. 5. SEM images of Bi$_2$S$_3$: (a) obtained from complex **6** and (b) obtained from complex **8** refluxing in xylene.
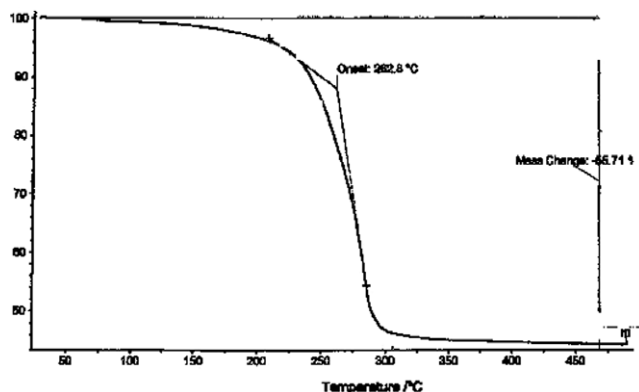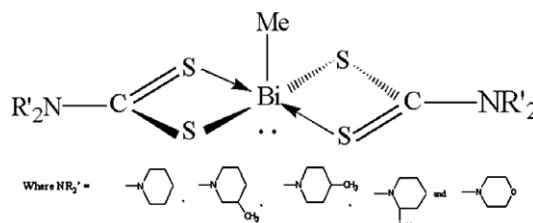

Fig. 6. TG curve of complex(6).

by the S atoms of the two aniso-bidentate ligands in which one of the Bi–S bonds tends to be distinctly shorter (ave 2.72(2) Å) than the other (ave 3.00(2) Å). The same phenomenon was noted for the xanthate ligands in MeBi(S$_2$COMe)$_2$ [7]. By contrast, in **2** the ligand is truly bidentate with similar, relatively short Bi(1)–S(1) and Bi(1)–S(2) distances (2.670(2) and 2.679(2) Å) that are close to the sum of the covalent radii of Bi and S of 2.63 Å. The average Bi–Cl distance of

Fig. 7. Proposed structure of the complexes [MeBi(S$_2$CNR′$_2$)$_2$].

products of various structural properties. The X-ray structure of [MeBiCl(S$_2$CNEt$_2$)] reveals a polymeric structure arising from Bi···Cl···Bi bridging interactions and that the ligand is bidentate. On the basis of spectral studies, it is reasonable to conclude that all of these ligands behave in the same manner with bidentate attachment to the metal in methylbismuth(III)bis(dithiocarbamates) and the following tentative structures may be proposed for these types of derivatives (Fig. 7).

5. Supplementary material

Crystallographic data for the structural analysis has been deposited with the Cambridge Crystallographic Data Centre, CCDC No. 290340 for MeBiCl(S$_2$CNEt$_2$). Copies of this information may be obtained free of charge from the Director, CCDC, 12 Union Road, Cambridge, CB2 1EZ, UK, fax: +44 1223 336033; email: deposit@ccdc. cam.ac.uk or www: http://www.ccdc.cam.ac.uk.

Acknowledgements

References

[1] P. Lostak, A. Drasar, A. Krejcova, L. Benes, J.S. Dyek, W. Chen, C. Uher, J. Cryst. Growth 222 (2001) 565.
[2] O. Salminen, A. Ozoles, P. Riihola, P. Moenkkoenn, J. Appl. Phys. 78 (1983) 718.
[3] I. Haiduc, C. Silvestru, Coordin. Chem. Rev. 99 (1990) 253.
[4] B.K. Keppler, C. Silvestru, I. Haiduc, Met.-Based Drugs 1 (1994) 75.
[5] S.S. Garje, V.K. Jain, Coordin. Chem. Rev. 236 (2003) 35.
[6] G.G. Briand, N. Burford, Chem. Rev. 99 (1999) 260.
[7] A. Gupta, R.K. Sharma, R. Bohra, V.K. Jain, J.E. Drake, M.B. Hoursthouse, M.E. Light, J. Organomet. Chem. 678 (2003) 122.
[8] S.S. Garje, V.K. Jain, E.R.T. Tiekink, J. Organomet. Chem. 538 (1997) 129.
[9] H. Althaus, H.J. Breunig, E. Lork, Organometallics 20 (2001) 586.
[10] Z. Otwinowski, W. Minor, DENZO data collection and processing software, in: C.W. CarterJr., R.M. Sweet (Eds.), Methods in enzymology, Macromolecular Crystallography, Part A, vol. 276, Academic press, 1997, pp. 307–326.
[11] G.M. Sheldrick, Acta Crystallogr. A 46 (1990) 467.
[12] L.J. Farrugia, J. Appl. Cryst. 32 (1999) 837.
[13] G.M. Sheldrick, SHELXL 97, University of Gottingen, Germany.
[14] E. Brau, R. Falke, A. Ellner, M. Beuter, U. Kolb, M. Drager, Polyhedron 13 (1994) 365.
[15] Powder Diffraction File No. 17-320, compailed by JPCDS, International centre for diffraction data, USA, 1986.
[16] C. Burschka, M. Wieber, Z. Naturforsch, Teil B. 34 (1979) 1037.